CONF-960202--12

LA-UR-96- 0140

Title: MICROSTRUCTURES AND ELECTRICAL PROPERTIES OF $SrRuO_3$ THIN FILMS ON $LaAlO_3$ SUBSTRATES

Author(s):
F. Chu - CMS
T. E. Mitchell - CMS
M. Hawley - CMS
G. Landrum - CMS
Q. X. Jia - STC
X. D. Wu - STC

Submitted to: Journal Elec. Mat.
Invited paper at 125th TMS Annual Meeting
Anaheim, CA
Feb. 4 - Feb. 8, 1996

Los Alamos
NATIONAL LABORATORY

Form No. 836 R5
ST 2629 10/91

Microstructures and Electrical Properties of $SrRuO_3$ Thin Films on $LaAlO_3$ Substrates

F. Chu, Q. X. Jia, G. Landrum*, X. D. Wu, M. Hawley, and T. E. Mitchell
Materials Science and Technology Division, Los Alamos National Laboratory, Los Alamos, NM 87545, U. S. A.

Abstract

Conductive oxide $SrRuO_3$ thin films have been deposited using pulsed laser deposition on $LaAlO_3$ substrates at different substrate temperatures. Structural and microstructural properties of the $SrRuO_3/LaAlO_3$ system have been studied using x-ray diffraction, scanning electron microscopy and scanning tunneling microscopy. Electrical properties of $SrRuO_3$ thin films have been measured. It was found that the film deposited at 250°C is amorphous-like, showing semiconductor-like temperature dependence of electrical conductivity. The film deposited at 425°C is crystalline with very fine grain size (100~200Å), showing both metallic and semiconductor-like temperature dependence of the electrical conductivity in different temperature regions. The film deposited at 775°C shows a resistivity of 280 μΩ.cm at room temperature and the residual resistivity ratio of 8.4. The optimized deposition conditions to grow $SrRuO_3$ thin films on $LaAlO_3$ substrates have been found. Possible engineering applications of $SrRuO_3$ thin films deposited at different temperatures are discussed. Bulk and surface electronic structures of $SrRuO_3$ are calculated using a semi-empirical valence electron linear combination of atomic orbitals approach. The theoretical calculation results are employed to understand the electrical properties of $SrRuO_3$ thin films.

*Present address: Department of Chemistry and Materials Science Center, Cornell University, Ithaca, New York, 14853-1301, U. S. A.

Introduction

Conductive solids are very useful in electronic devices, serving as contacts, metallization, and interconnects. Except metals, some oxides are metallic, while most are insulating [1]. Among conductive oxides, $SrRuO_3$, which crystallizes in perovskite structure with lattice parameters of a=0.556 nm, b=0.555 nm, and c=0.786 nm, has recently been found possible engineering applications in different fields. For example, the relatively high conductivity and structural compatibility of $SrRuO_3$ with ferroelectric or high dielectric constant materials make it promising as a bottom electrode for dynamic random memory capacitors [2-5]. In addition, highly thermal and chemical stabilities of $SrRuO_3$ make it attractive as a buffer layer for growth of high-temperature superconductor $YBa_2Cu_3O_{7-\delta}$ thin films on different substrates [6-7].

It has been observed experimentally that the electrical resistivity of bulk $SrRuO_3$ is a strong function of microstructure. Polycrystalline $SrRuO_3$ has a resistivity of 1130 $\mu\Omega$.cm at room temperature [8] whereas single crystalline $SrRuO_3$ has a room temperature resistivity of 280 $\mu\Omega$.cm [9]. $SrRuO_3$ thin films have been deposited using either off-axis sputtering or pulsed laser deposition on different substrates, e.g. $SiTiO_3$ [10], $LaAlO_3$ [3,6], MgO with Pt or $BaTiO_3$ [4,7] buffer layer, and Si with yttria stabilized zirconia (YSZ) as a buffer layer [5]. However, microstructural and electrical properties of these $SrRuO_3$ thin films have not been systematically studied. This investigation is crucial for $SrRuO_3$ thin films to be used as a bottom electrode in microelectronic devices, because the device performance is strongly related to the microstructure and electrical resistivity of the films.

It is our intent, in this paper, to study the relationship between the microstructures and electrical properties of $SrRuO_3$ thin films deposited on a specific substrate, $LaAlO_3$, at different substrate temperatures. In Section 2, the experimental procedure and calculation method are described. The experimental results on microstructures and electrical properties and the calculation results are presented and discussed in Section 3. Conclusions are drawn in Section 4.

Experimental Procedures and Calculation Method

Pulsed laser deposition (PLD) with a XeCl excimer laser (λ=3008Å) was used to deposit $SrRuO_3$ thin films on $LaAlO_3$ substrates. The $SrRuO_3$ target was prepared by mixing appropriate molar ratios of $SrCO_3$ and Ru metal powder, grinding, heating in air at 1200 °C for 12 hours, regrinding and heating, and repressing into disks [6]. Single crystal (100) $LaAlO_3$ (a=0.3793 nm) wafers were employed as substrates. Before deposition, the substrates were cleaned in a sequence of acetone, methanol, and deionized water. In the deposition process, the *in situ* PLD operated at an energy density of 2 J/cm^2 and repetition rates of 10-20 Hz. The oxygen pressure was experimentally optimized and maintained at 200 mTorr during film deposition in order to keep the stoichiometry of the films. The deposition temperatures were varied from room temperature to 850 °C. The nominal film thickness was in the range of 100 - 1500 nm.

The structural properties of the $SrRuO_3$ thin films were characterized using a combination of x-ray diffraction (XRD), scanning electron microscopy (SEM), and scanning tunneling microscopy (STM). A Siemens D5000 four circle x-ray diffractometer with Cu K_α radiation was employed to examine the crystallographic orientation and crystallinity of the thin films. A JEOL JSM-6300FXV field emission gun scanning electron microscope was used to study the surface morphology and microstructure of the thin films. A Nanoscope III STM was employed to measure the surface roughness of the thin films.

The electrical properties of the thin films were studied by measuring their electrical resistivity. The resistivity of the $SrRuO_3$ thin films was measured using a standard four-probe technique, in which the $SrRuO_3$ thin films were patterned by ion milling to form a bridge of 500 µm in width and 2.5-7.5 mm in length. Au contact pads were deposited on the patterned $SrRuO_3$ thin films by rf sputtering in vacuum.

The electronic structures of the bulk and surface of $SrRuO_3$ were calculated using the extended Hückel implementation of the tight-binding method. The extended Hückel theory is a semi-empirical valence electron Linear Combination of Atomic Orbitals (LCAO) approach [11]. The band

structure and the density of states of the bulk and thin film of $SrRuO_3$ were obtained, which can be used to understand the electrical conducting behavior of the systems. The details of the calculations will be published elsewhere [12].

Results and Discussion

1. *Structural Properties of $SrRuO_3$ Thin Films*

XRD pattern of θ-2θ scan on the $SrRuO_3$ thin film deposited at 775°C on a $LaAlO_3$ substrate is shown in Fig. 1. Note that for $SrRuO_3$, the lattice parameters satisfy a~b and a~b~c/$\sqrt{2}$, so the (220) and (004) peaks may overlap. Therefore, Figure 1 shows that the $SrRuO_3$ thin film is **c**-axis or/and **a**+**b**-axis oriented with respect to the substrate normal. The detailed crystallographic study using transmission electron microscopy for this feature of the system will be published elsewhere [13]. Figure 2 demonstrates the XRD ω-rocking curve of the (004)/(220) reflection of the $SrRuO_3$ thin film, showing that the full width at half maximum (FWHM) is about 0.72°. The very narrow ω-rocking curve suggests that the $SrRuO_3$ thin film deposited at 775°C is well **c**-axis or/and **a**+**b**-axis oriented with respect to the substrate. The in-plane orientation of the $SrRuO_3$ film with respect to the (100) $LaAlO_3$ substrate is measured by XRD φ-scan on both the $SrRuO_3$ (404) and the $LaAlO_3$ (101) reflections. Figure 3 shows the typical XRD φ-scans on both the (404) reflection of the $SrRuO_3$ thin film deposited at 775°C and the (101) reflection of the $LaAlO_3$ substrate. It is reasonable to have the 45° rotation between the basal plane of $SrRuO_3$ and that of $LaAlO_3$, as shown in Fig. 3, because the compatibility of the lattice parameters of the two systems: $a_{SrRuO_3} \sim a_{LaAlO_3}\sqrt{2}$. The lattice mismatch is less than 4% with such a growth pattern [$\langle 001 \rangle_{SrRuO_3} // \langle 011 \rangle_{LaAlO_3}$ and $(001)_{SrRuO_3} // (100)_{LaAlO_3}$].

The effect of deposition temperature on the crystallinity of the $SrRuO_3$ thin films can be demonstrated by the plot of the FWHM values of both the ω-rocking curve on the (004)/(220) reflection and the φ-scan on the (404) reflection of the $SrRuO_3$ films deposited at different temperatures. Figure 4 shows the values of these FWHMs of the $SrRuO_3$ thin films as a function of deposition temperature. It can be seen from Fig.

4 that the values of the FWHM decrease monotonically with increasing deposition temperature. It is physically plausible to have smaller FWHMs, i.e., better crystallized thin films, at higher deposition temperatures. However, it is remarkable that well aligned $SrRuO_3$ thin films can be grown on $LaAlO_3$ substrates by PLD at a deposition temperature as low as 450°C. It is possible that the energetic ions in the laser plume enhance the texture of the thin films, compensating for the lack of sufficient thermal energy supplied by the low temperature substrates. In addition, it is expected based on Fig. 4 that the optimized $SrRuO_3$ thin films in terms of crystallinity can be grown in the range of 650-800°C.

The degree of the crystallinity of the $SrRuO_3$ thin films grown on $LaAlO_3$ substrates can also be studied by SEM. Figure 5 shows the surface morphology and microstructure of the $SrRuO_3$ thin films deposited on $LaAlO_3$ at different temperatures. First of all, it can be seen from Fig. 5 that the surfaces of the films deposited at different substrate temperatures are very clean and smooth, and no particles are detected. The smoothness of the film makes the $SrRuO_3$ system very promising as a bottom electrode material in high capacity thin film capacitors because of the lack of microshort from the particles. Furthermore, it can be seen from Fig. 5 that the grain size of the films increases with increasing deposition temperature. Epitaxial growth of $SrRuO_3$ on $LaAlO_3$ by PLD occurs at deposition temperatures higher than 650°C [13], although a well textured $SrRuO_3$ film can be obtained at a deposition temperature as low as 450°C.

Finally, the smoothness of the thin films can be quantitatively measured by STM. Figure 6 shows the r.m.s. surface roughness of the $SrRuO_3$ thin films on $LaAlO_3$ deposited at different temperatures. It can be seen from Fig. 6 that the $SrRuO_3$ thin films deposited at temperatures higher than 650°C are extremely smooth, having r.m.s. surface roughness less than 0.2 nm within a testing area of 0.1x0.1 μm^2.

2. *Electrical Properties of $SrRuO_3$ Thin Films*

Room-temperature electrical resistivities of the $SrRuO_3$ thin films deposited at different substrate temperatures by PLD are shown in Fig. 7. It can be seen from Fig. 7 that the deposition temperature has a strong

impact on the room temperature resistivity of the $SrRuO_3$ thin films. The higher the deposition temperature of the films, the more conductive the films are. The room temperature resistivity decreases more than three orders in magnitude when the deposition temperature increases from 250°C to 775°C. The $SrRuO_3$ thin film deposited at 775°C by PLD with the optimized crystal structure is highly conductive with a room temperature resistivity of around 280 μΩ.cm. This value is very close to that of bulk single crystal $SrRuO_3$ [9], lower than 340 μΩ.cm of sputtered $SrRuO_3$ films [10], and much lower than 1130 μΩ.cm of bulk polycrystalline $SrRuO_3$ [8]. It is physically plausible to believe that the room temperature resistivity of the $SrRuO_3$ thin films is directly related to the crystallinity of the films, because, as analyzed above, deposition temperature has a strong influence on the crystallinity of the films. It has been shown above that the crystallinity of the films increases with increasing deposition temperature and the $SrRuO_3$ thin films become highly textured when deposited above 450°C. It is especially worthwhile to note that the grain size of the films increases with increasing deposition temperature, as shown in Fig. 5. It is believe that the reduced grain boundary scattering from crystallized films enhances the conductivity of the films. On the other hand, the room temperature resistivity of the polycrystalline $SrRuO_3$ can be as high as 1130 μΩ.cm, presumably due to strong grain boundary scattering. Therefore, it is very clear that only the crystalline-like $SrRuO_3$ thin films should be used as electrode materials, and the other forms, either polycrystalline or amorphous, are of too high resistivity and should be excluded from consideration. In addition, a very weak dependence of the film resistivity on the oxygen pressure during film deposition in the range of 50 to 200 mTorr for a given deposition temperature indicates that the films are completely oxidized under our optimized PLD process conditions.

Temperature dependence of the electrical resistivity of the films deposited at different substrate temperatures by PLD is shown in Fig. 8. It can be seen from Fig. 8 that the films deposited at different substrate temperatures have different temperature dependence of electrical resistivity (ρ-T characteristic). The $SrRuO_3$ films deposited at 250°C has a semiconductor-like characteristic in resistivity, as shown in Fig. 8 (a).

However, the ρ-T characteristic is composed of three distinguished regions if the $SrRuO_3$ thin film is deposited at 450°C, as shown in Fig. 8 (b). The ρ-T curve of the film is semiconductor-like below 93K, metallic-like in the range of 93K to 160K, and virtually constant above 160K. The $SrRuO_3$ films deposited above 650°C show metallic resistivity vs. temperature behavior, where the kink at about 160 K represents the Curié point of $SrRuO_3$ which becomes ferromagnetic below this temperature [14]. These unique ρ-T characteristics of the $SrRuO_3$ thin films deposited at certain temperatures may provide new features in development of novel electronic devices. Further work is underway to investigate such properties on the $SrRuO_3$ thin films.

Another well-known direct measurement of film perfection, the residual resistivity ratio (RRR), is also studied for the $SrRuO_3$ thin films. Based on the analysis of temperature dependence of resistivity, it is found that the RRR of $SrRuO_3$ thin films on $LaAlO_3$ substrates increases with increasing deposition temperature. The RRR of the $SrRuO_3$ films is 3.4 and 8.4, respectively, while increasing deposition temperature from 650°C to 775°C. Note that a RRR of around 12 has been reported for bulk single crystalline $SrRuO_3$ [9] and a RRR of less than 3 has been measured for $SrRuO_3$ thin films epitaxially grown by sputtering [10]. The higher RRR value for the PLD deposited $SrRuO_3$ thin films on $LaAlO_3$ substrates can be attributed to the higher crystallinity of the films at higher deposition temperatures by PLD.

3. *Theoretical Calculations*

Although it has been experimentally found that bulk $SrRuO_3$, as one of few conductive oxides, is electrically conductive, the physical mechanism for conductivity has never been explained based on electronic structure calculations. Figure 9 (a) shows the total density of states (DOS) for bulk $SrRuO_3$ in the experimental geometry, while Fig. 9 (b) shows the energy levels of the $[Ru(OH)_6]^{2-}$ model of the Ru coordination environment in $SrRuO_3$. It can be seen from Fig. 9 that the Fermi level of bulk $SrRuO_3$ cuts through the conduction band, so that the DOS at Fermi level, $N(E_F)$, is of a significant value, i.e. the bulk $SrRuO_3$ is electrically conductive. In addition, the contribution of the d-electrons from Ru substantially

determines the conductivity of bulk $SrRuO_3$. However, the $N(E_F)$ is not very high, as shown in Fig. 9, therefore, it is expected that bulk $SrRuO_3$ still has a relatively high resistivity at room temperature (280 $\mu\Omega$.cm).

In order to study the electrical properties of $SrRuO_3$ thin films, the electronic structure of the $SrRuO_3$ (001) surface was determined using a two dimensional slab model. This model used a slab made up of five atomic planes: RuO_2-SrO-RuO_2-SrO-RuO_2. The total DOS and projected DOS of the surface atoms is shown in Fig. 10. The most striking features can be seen from Fig. 9 and 10 are that the DOS of the $SrRuO_3$ (001) slab is very similar to that of the bulk $SrRuO_3$ and the position of Fermi level, E_F, of the $SrRuO_3$ (001) slab is almost the same as that of the bulk $SrRuO_3$. The major difference is the presence of the peak appearing below -12 eV in $SrRuO_3$ (001) slab, which is composed almost entirely of surface states. These are the so-called "dangling bonds" states which arise when the bulk material is cleaved and some bonds are broken. Due to the fact that these states appear ~1 eV above E_F (which is still in much the same position as it is in the bulk), we would not expect the conductivity of this perfect $SrRuO_3$ (001) surface to be significantly different from that of the bulk.

It is very important to point out that the model system employed in these slab calculations are much thinner than the films reported in this work (100-150 nm). In a real $SrRuO_3$ thin film, there are many more layers, this would give rise more bulk-like electronic structure and electrical behavior. Since there is no significant perturbation of the DOS near E_F by the formation of the $SrRuO_3$ (001) surface, we would expect these films with the optimized crystal structure to exhibit a conductivity close to that of the bulk single crystalline $SrRuO_3$, as pointed out above based on the experimental results. Furthermore, we do not believe that the observed semiconductor-like and temperature-independent behavior of the $SrRuO_3$ thin films deposited at certain temperatures can be explained in terms of the electronic structure of a perfect film. These anomalous electrical properties of $SrRuO_3$ thin films must be due to more macroscopic phenomena, such as grain boundary scattering.

Conclusions

The structural and electrical properties of $SrRuO_3$ thin films deposited on $LaAlO_3$ at different substrate temperatures by PLD have been studied. The following conclusions can be drawn from the investigation:

(1) Microstructure dependence on deposition temperatures has been revealed. The films have a better crystallinity, i.e. higher textured crystalline with a larger grain size and a smaller surface roughness, when grown at higher deposition temperatures. Although a well aligned $SrRuO_3$ thin film can be grown at 450°C, the optimized $SrRuO_3$ thin films on $LaAlO_3$ substrates should be grown by PLD at above 650°C.

(2) Room temperature resistivity dependence on deposition temperature has been examined. The $SrRuO_3$ thin film deposited at 775°C has an optimized electrical resistivity of 280 μΩ.cm, which is very close to that of the bulk single crystalline $SrRuO_3$. It also has a RRR value of 8.4, which is much higher than those of polycrystalline bulk and sputterly grown thin film $SrRuO_3$. In addition, it has the lowest surface roughness. All of these make this optimized film a very attractive bottom electrode material.

(3) Temperature dependence of electrical resistivity (ρ-T characteristic) of the $SrRuO_3$ thin films deposited at different substrate temperatures has been determined. The $SrRuO_3$ films deposited at 250°C has a semiconductor-like characteristic in resistivity. However, the ρ-T characteristic is composed of three distinguished regions if the $SrRuO_3$ thin film is deposited at 450°C: semiconductor-like below 93K, metallic-like in the range of 93K to 160K, and virtually temperature-independent above 160K. The $SrRuO_3$ films deposited above 650°C show metallic behavior, where the kink at about 160 K represents the Curié point of $SrRuO_3$. These unique ρ-T characteristics of the $SrRuO_3$ thin films deposited at certain temperatures may provide new features in fabrication of novel electronic devices.

(4) The electronic structures of the bulk and (001) slab of $SrRuO_3$ have been calculated using the extended Hückel implementation of the tight-binding method. Electrons of $SrRuO_3$ perovskite fill the Fermi surface in

such a way that $N(E_F)$ is of a significant value, which results in the conductivity of $SrRuO_3$. More importantly, the DOS and the position of Fermi level of thin film and bulk $SrRuO_3$ are basically the same, which result in the conductivity of thin film close to that of bulk single crystals. Furthermore, anomalous electrical properties of the $SrRuO_3$ thin films grown at different deposition temperatures should be understood in terms of more macroscopic phenomena, such as grain boundary scattering, instead of electronic structure.

Acknowledgment

This research was supported by the U. S. Department of Energy. Helpful discussion with C. D. Adams is appreciated.

References

[1] J. B. Torrance, P. Lacorre, C. Asavaroengchai, and R. M. Metzger, *Physica* C **182**, 351 (1991).

[2] C. B. Eom, R. B. van Dover, J. M. Phillips, D. J. Werder, J. H. Marshall, C. H. Chen, R. J. Cava, R. M. Fleming, and D. K. Fork, *Appl. Phys. Lett.* **63**, 2570 (1993).

[3] Q. X. Jia, X. D. Wu, S. R. Foltyn, and P. Tiwari, *Appl. Phys. Lett.* **66**, 2197 (1995).

[4] L. A. Wills and J. Amano, *MRS Symp. Proc.* Vol. **361**, 470 (1995).

[5] S. Y. Hou, J. Kwo, R. K. Watts, J. Y. Cheng, and D. K. Fork, Appl. Phys. Lett., **67**, 1387 (1995).

[6] X. D. Wu, S. R. Foltyn, R. C. Dye, Y. Coulter, and R. E. Muenchausen, *Appl. Phys. Lett.* **62**, 2434 (1993).

[7] P. Tiwari, X. D. Wu, S. R. Foltyn, M. Q. Le, I. H. Campbell, R. C. Dye, and R. E. Muenchausen, *Appl. Phys. Lett.* **64**, 634 (1994).

[8] Y. Nora and S. Miyahara, *J. Phys. Sco. Jpn.* **27**, 518 (1969).

[9] R. J. Bouchard and J. L. Gillson, *Mater. Res. Bull.* **7**, 873 (1972).

[10] C. B. Eom, R. J. Cava, R. H. Fleming, J. M. Phillips, R. B. van Dover, J. H. Marshall, J. W. P. Hsu, J. J. Krajewski, and W. F. Peck, Jr., *Science* **258**, 1766 (1992).

[11] R. Hoffmann, *J. Chem. Phys.* **39**, 1397 (1963), **40**, 2474 (1964), and **40**, 2745 (1964).

[12] G. A. Landrum et al., to be published.

[13] Q. X. Jia, F. Chu, X. D. Wu, M. Hawley, J. H. Cho, S. R. Foltyn, J. L. Smith, and T. E. Mitchell, to be published.

[14] A. Callaghan, C. W. Moeller, and R. Ward, *Inorg. Chem.* **5**, 1572 (1966).

Figure Captions

Fig. 1 X-ray diffraction of θ-2θ scan on the $SrRuO_3$ thin film deposited at 775°C on a $LaAlO_3$ substrate.

Fig. 2 X-ray ω-rocking curve on the (004)/(220) reflection of the $SrRuO_3$ thin film deposited at 775°C on a $LaAlO_3$ substrate.

Fig. 3 X-ray diffraction φ-scans on both the (404) reflection of the $SrRuO_3$ thin film deposited at 775°C and the (101) reflection of the $LaAlO_3$ substrate.

Fig. 4 Crystallinity of the $SrRuO_3$ thin films as a function of deposition temperature, showing the FWHMs for the ω-rocking curve (tilt of **c**-axis or/and **a**+**b**-axis) on the $SrRuO_3$ (004)/(220) reflection and for the φ-scan (in-plane twist misaliognment) on the $SrRuO_3$ (404) reflection.

Fig. 5 SEM micrograph of the $SrRuO_3$ thin films on $LaAlO_3$ deposited at (a) 250°C, (b) 450°C, (c) 650°C, and (d) 775°C.

Fig. 6 Deposition temperature dependence of the surface roughness of the $SrRuO_3$ thin films.

Fig. 7 Room-temperature resistivity of the $SrRuO_3$ thin films as a function of depostion temperature.

Fig. 8 Temperature dependence of the normalized resistivity of the films deposited at different deposition temperatures: (a) 250°C, (b) 450°C, and (c) 650°C and 775°C.

Fig. 9 (a) Solid line: the total DOS for bulk $SrRuO_3$ in the experimental geometry . Filled area: the contribution of Ru to the tqtal DOS. The horizontal dashed line indicates the position of the calculated Fermi level (E_F). (b) The energy levels of the $[Ru(OH)_6]^{2-}$ model of the Ru coordination environment in $SrRuO_3$. Due to the small size of the distortion from octahedral coordination, many levels are nearly degenerate and appear as a single level.

Fig. 10 The calculated DOS of the 5 atomic layer model of the $SrRuO_3$ (001) surface. The shaded area indicates the contribution of surface atoms to the total DOS: (a) surface Ru's, (b) surface O's. The horizontal dashed line represents the position of Fermi level, E_F.

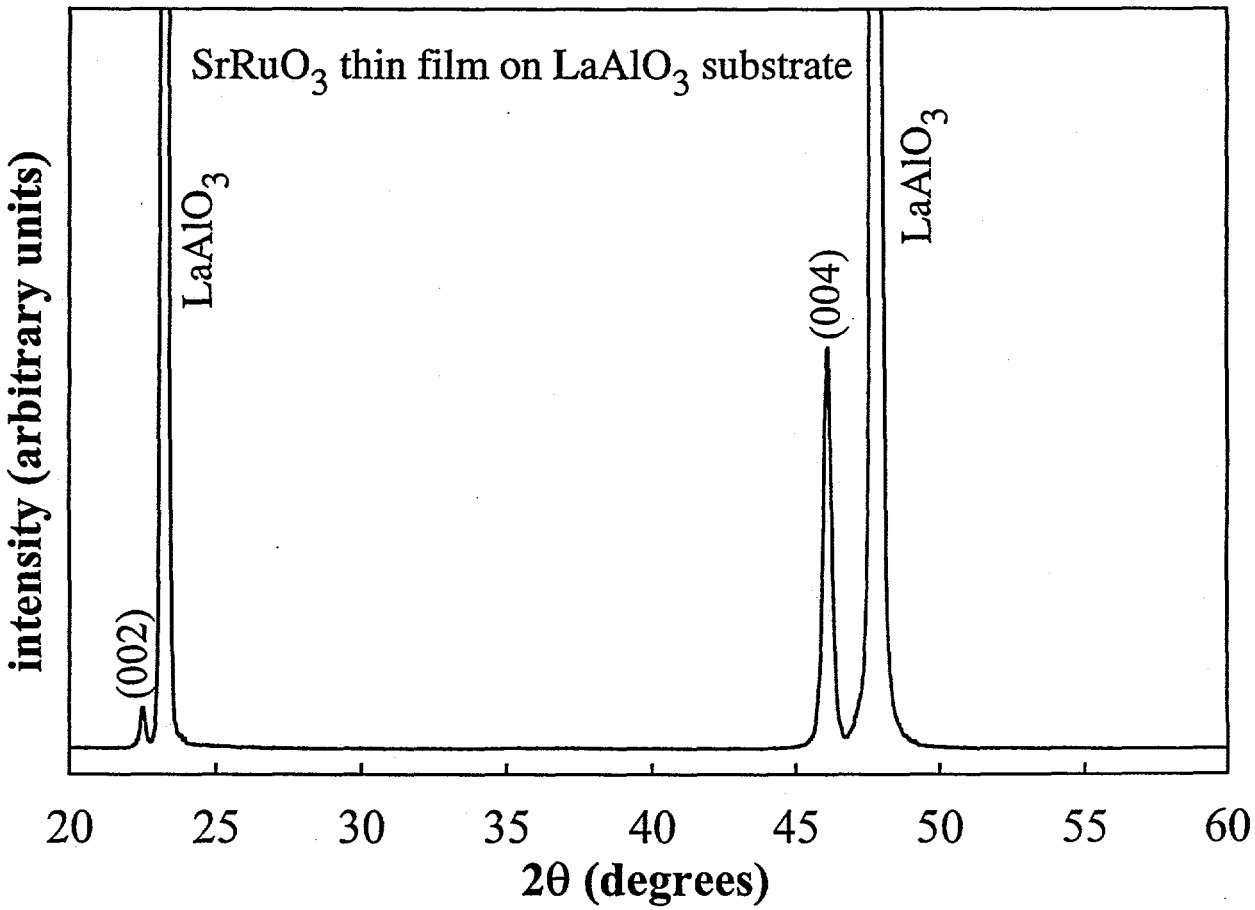
SrRuO3 thin film on LaAlO3 substrate
intensity (arbitrary units)
(002)
LaAlO3
(004)
LaAlO3
20
25
30
35
40
45
50
55
60
2θ (degrees)

Figure 1

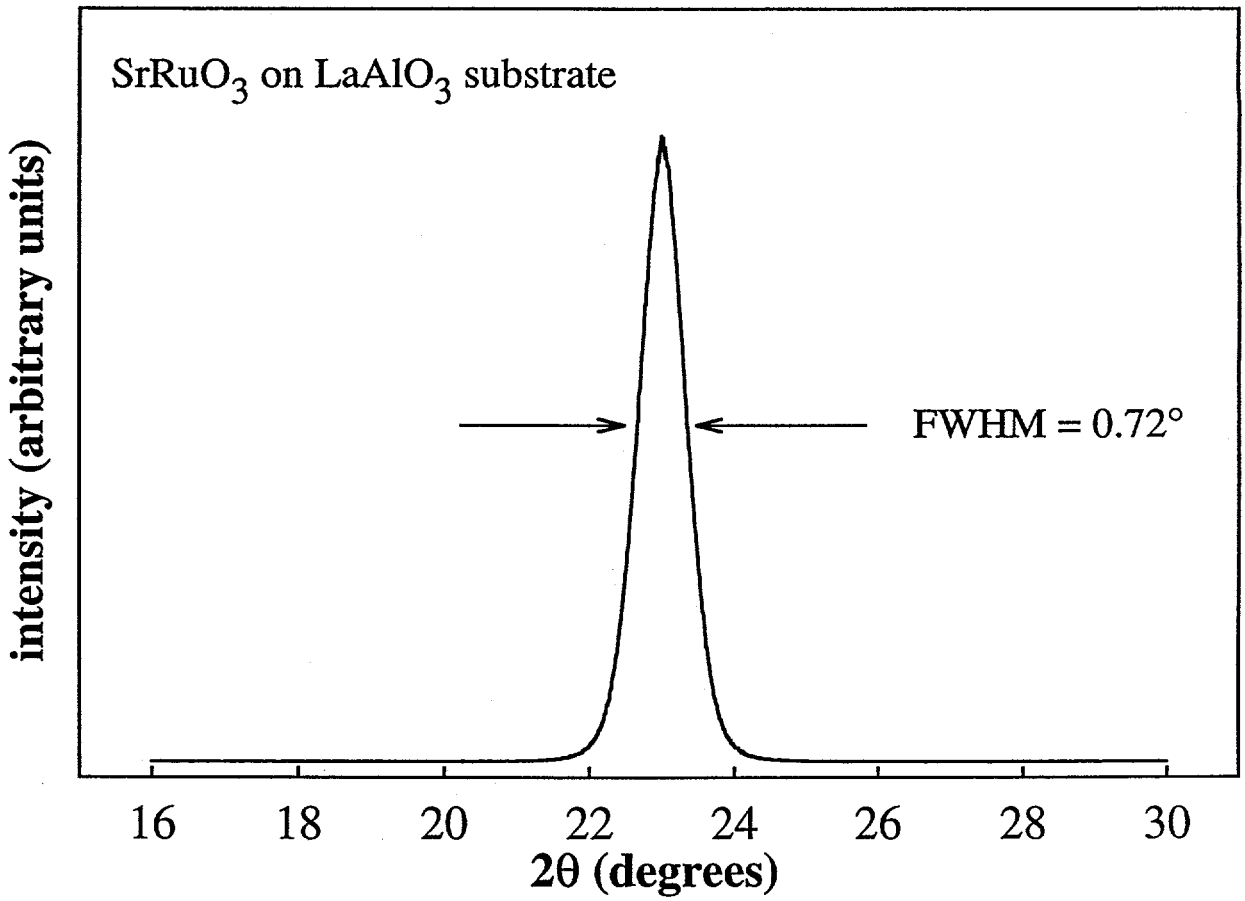
SrRuO3 on LaAlO3 substrate
intensity (arbitrary units)
FWHM = 0.72°
16
18
20
22
24
26
28
30
2θ (degrees)

Figure 2

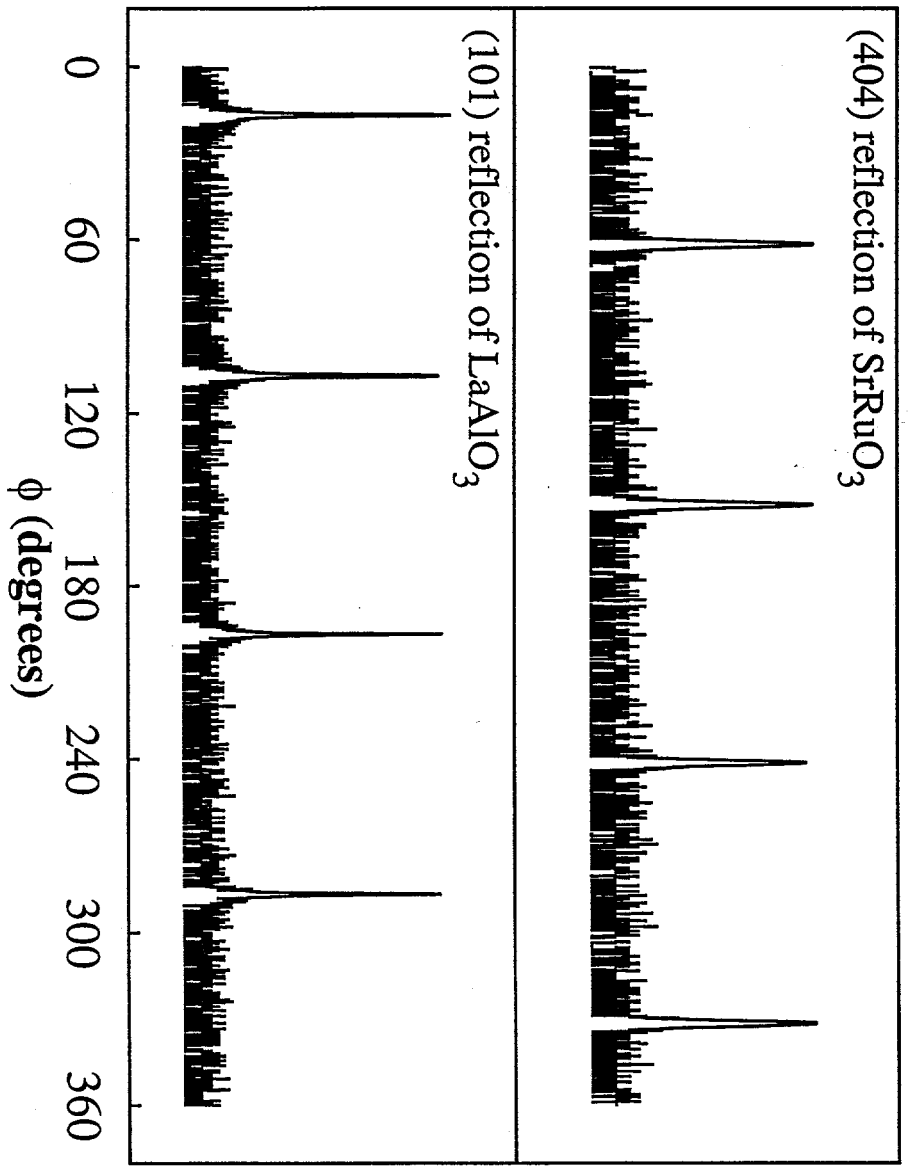
intensity/Log(Cps)
(404) reflection of $SrRuO_3$
(101) reflection of $LaAlO_3$
0
60
120
180
240
300
360
ϕ (degrees)

Figure 3

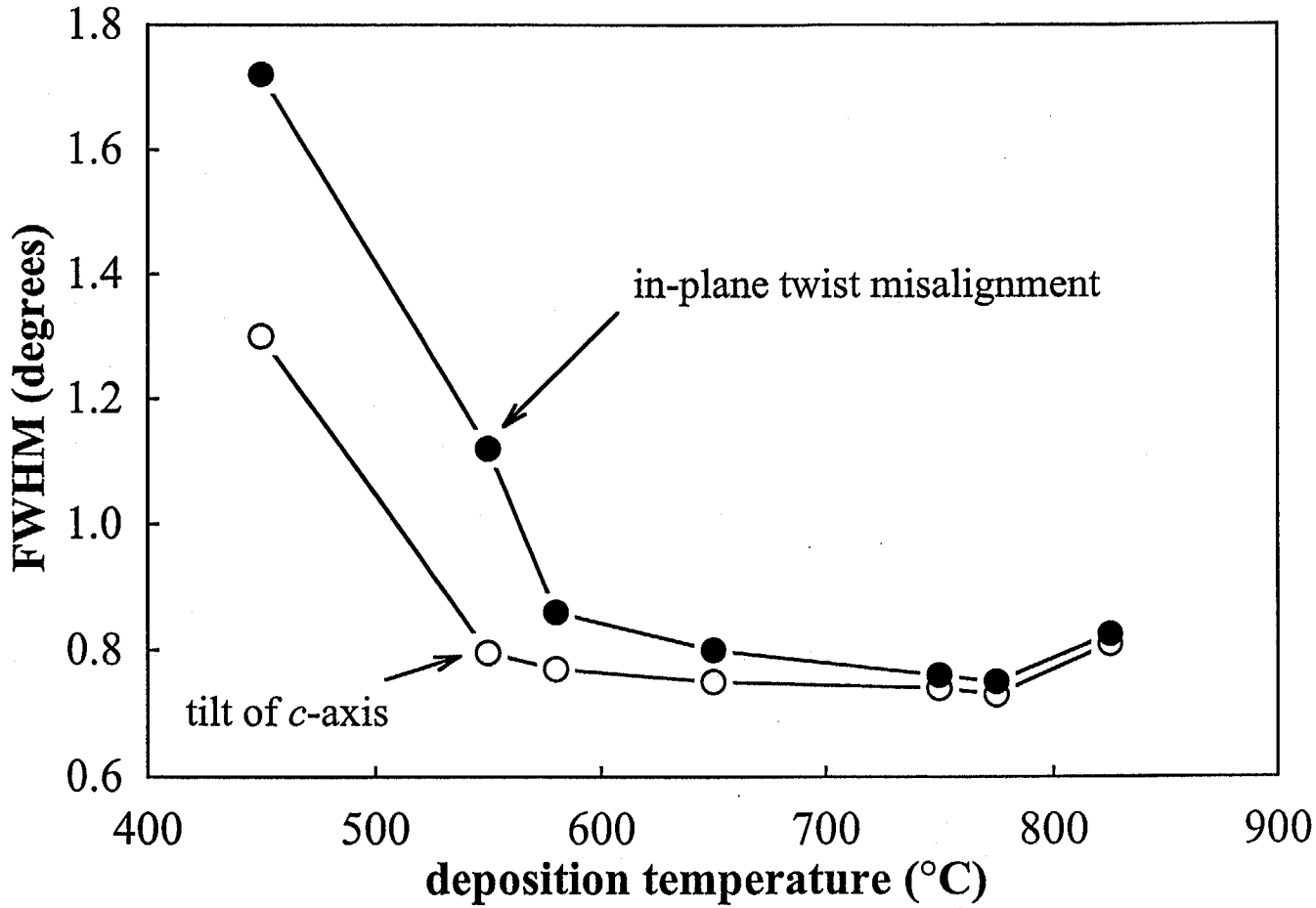
1.8
1.6
1.4
1.2
1.0
0.8
0.6
FWHM (degrees)
in-plane twist misalignment
tilt of c-axis
400
500
600
700
800
900
deposition temperature (°C)

Figure 4

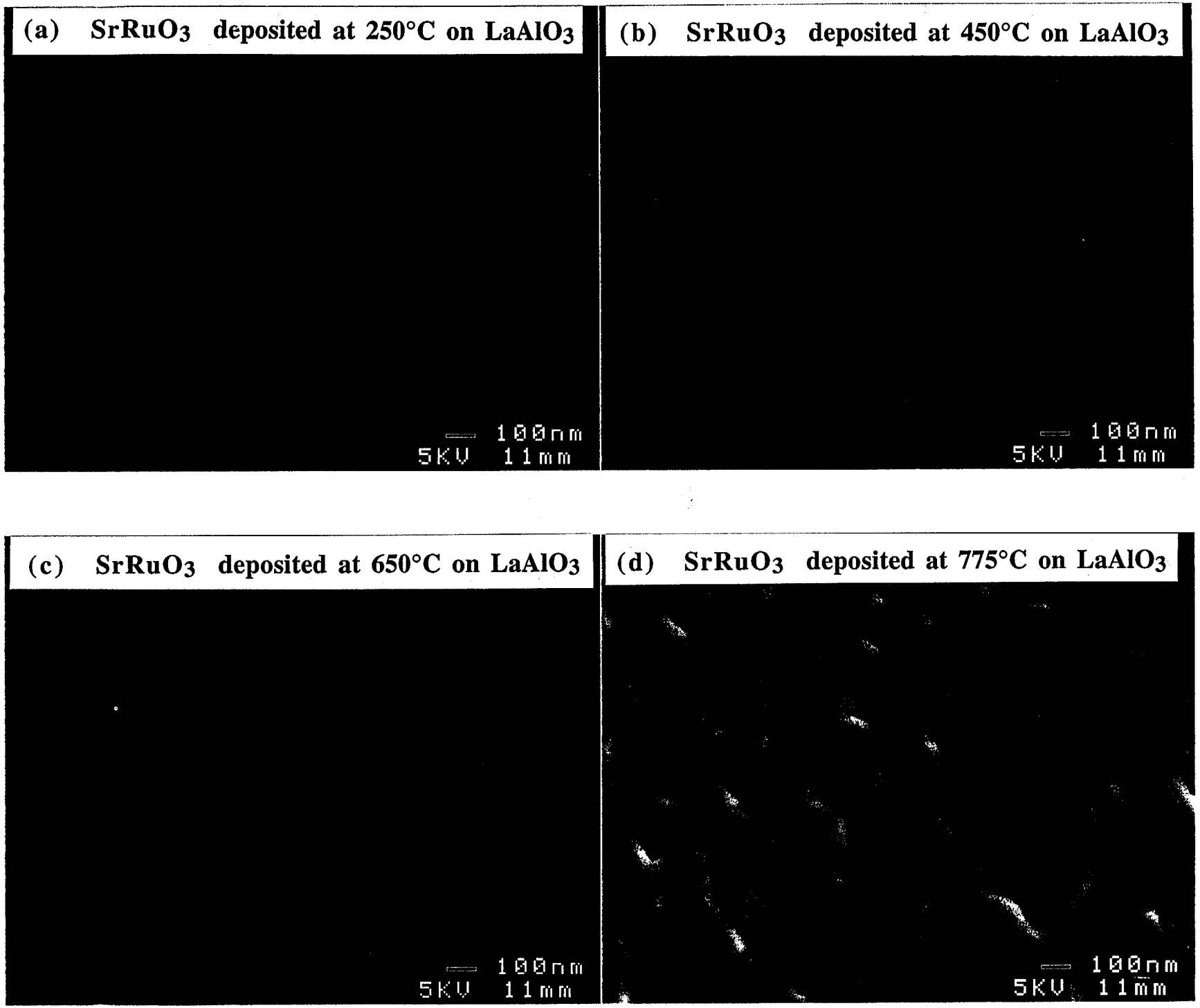
(a) SrRuO3 deposited at 250°C on LaAlO3
100nm
5KV 11mm
(b) SrRuO3 deposited at 450°C on LaAlO3
100nm
5KV 11mm
(c) SrRuO3 deposited at 650°C on LaAlO3
100nm
5KV 11mm
(d) SrRuO3 deposited at 775°C on LaAlO3
100nm
5KV 11mm

Figure 5

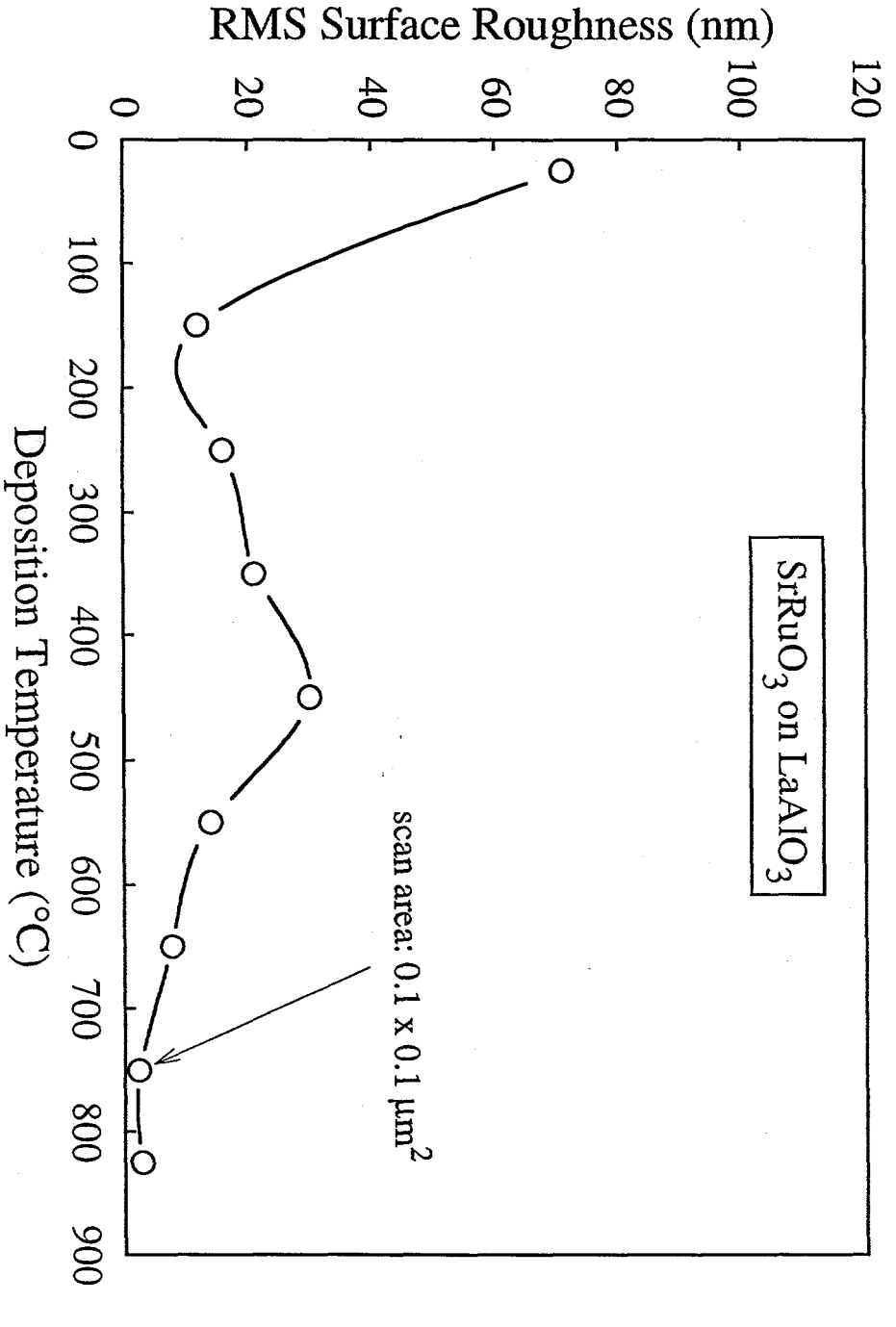
RMS Surface Roughness (nm)
0
20
40
60
80
100
120
0
100
200
300
400
500
600
700
800
900
Deposition Temperature (°C)
$SrRuO_3$ on $LaAlO_3$
scan area: 0.1 x 0.1 μm²

Figure 6

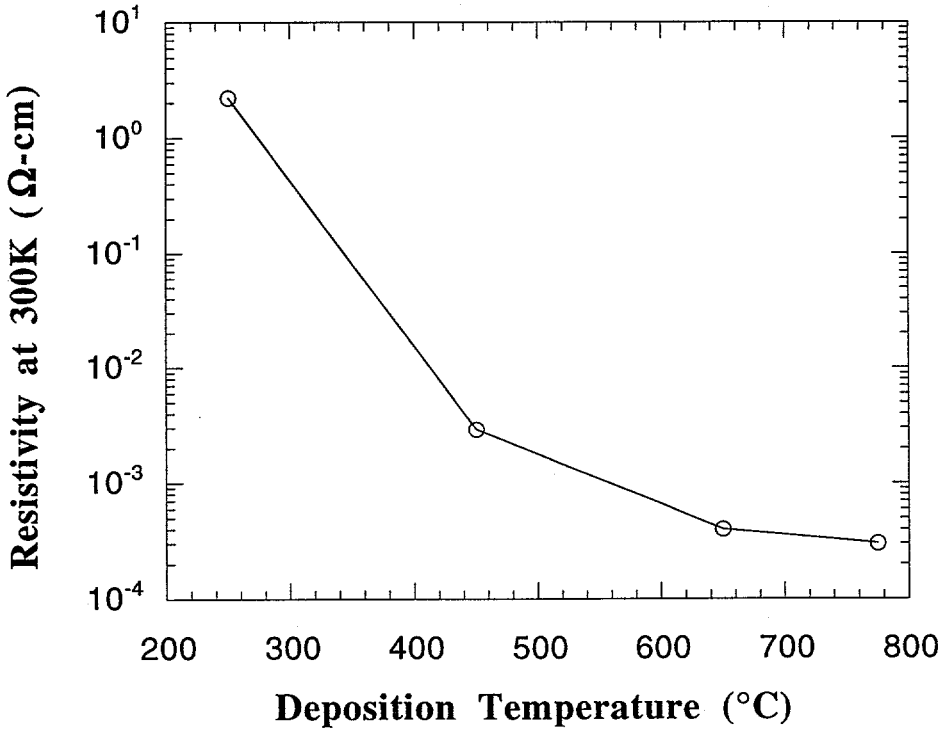
Resistivity at 300K (Ω-cm)
10^1
10^0
10^-1
10^-2
10^-3
10^-4
200
300
400
500
600
700
800
Deposition Temperature (°C)

Figure 7

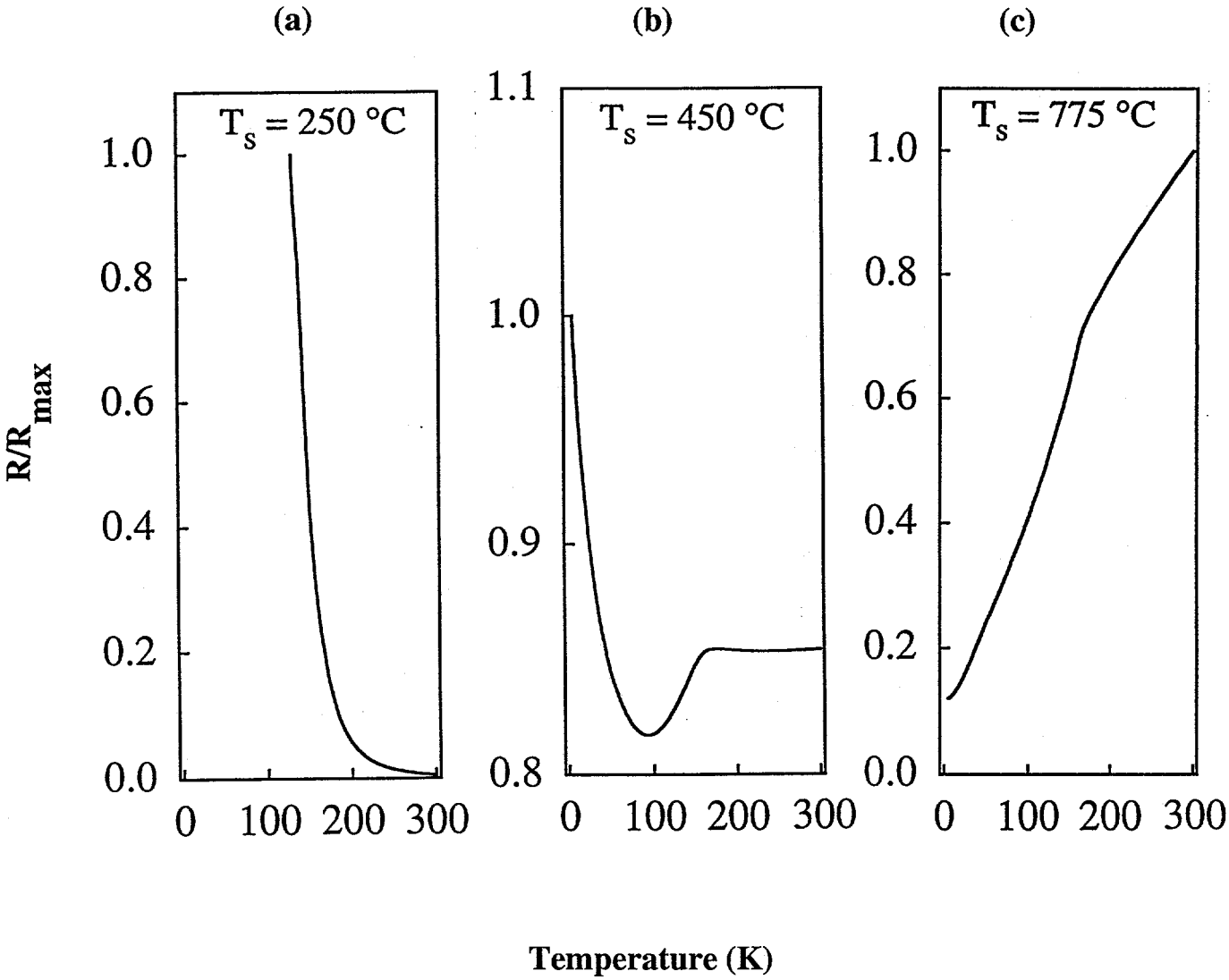
(a)
(b)
(c)
T_s = 250 °C
T_s = 450 °C
T_s = 775 °C
R/R$_{max}$
1.0
0.8
0.6
0.4
0.2
0.0
1.1
1.0
0.9
0.8
0 100 200 300
Temperature (K)

Figure 8

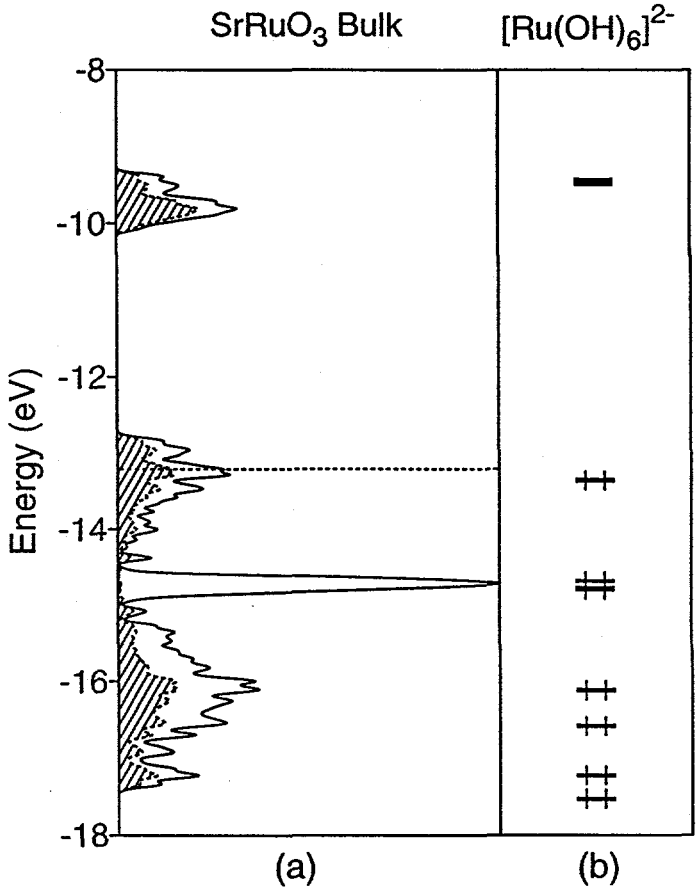

Figure 9

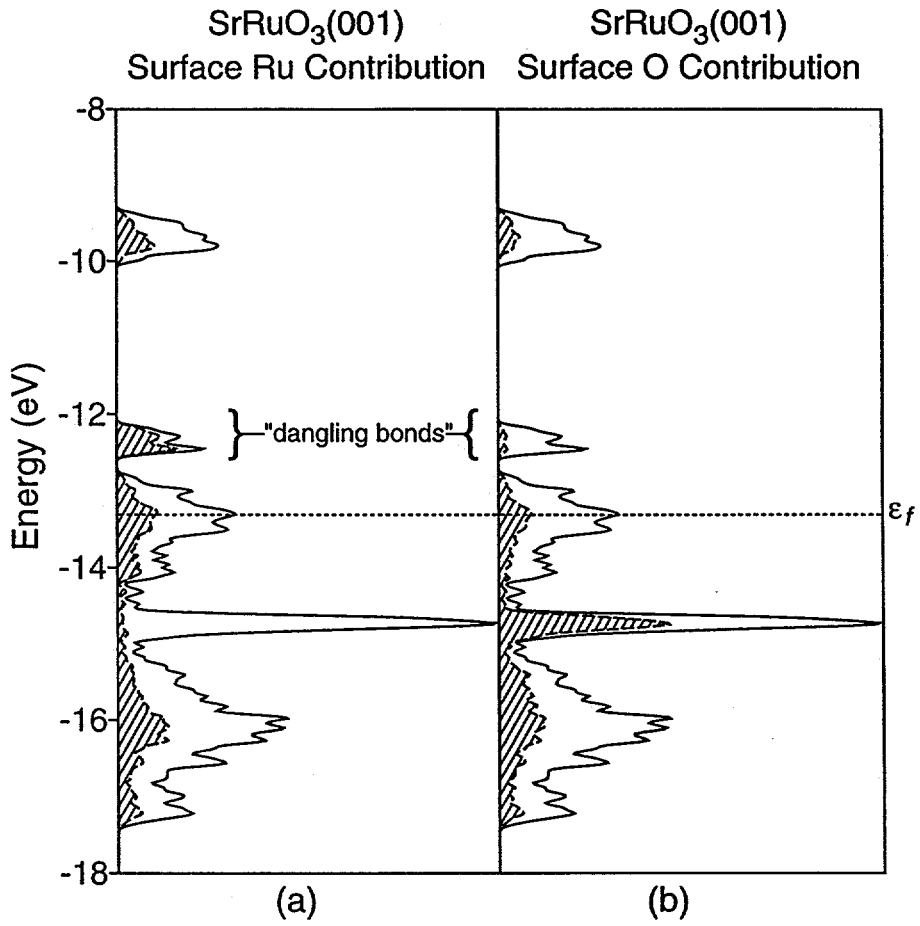
SrRuO3(001)
Surface Ru Contribution
SrRuO3(001)
Surface O Contribution
-8
-10
-12
-14
-16
-18
Energy (eV)
"dangling bonds"
εf
(a)
(b)

Figure 10